Title: Antibody responses to the Zika virus polyprotein in pregnant and non-pregnant macaques

Authors:

Emma L. Mohr[a]†, **Anna S. Heffron[b]†**, David Baker[b], Amelia K. Haj[b], Connor R. Buechler[b], Adam Bailey[b], Dawn M. Dudley[b], Christina M. Newman[b], Mariel S. Mohns[b], Michelle Koenig[b], Meghan E. Breitbach[b], Mustafa Rasheed[b], Laurel M. Stewart[b], Jens Eickhoff[c], Richard S. Pinapati[d], Erica Beckman[d], Hanying Li[d], Jigar Patel[d], John C. Tan[d], David H. O'Connor[b]#

Affiliations:

[a]Department of Pediatrics, School of Medicine and Public Health, University of Wisconsin-Madison

[b]Department of Pathology and Laboratory Medicine, University of Wisconsin-Madison

[c]Department of Biostatistics & Medical Informatics, University of Wisconsin-Madison

[d]Roche Sequencing Solutions, Madison

Running title: IgG responses to the ZIKV polyprotein in NHPs

#Address correspondence to David H. O'Connor, dhoconno@wisc.edu

†E.L.M and A.S.H. contributed equally to this work.

ABSTRACT

The kinetics and specificity of antibody responses against Zika virus (ZIKV) are not well-characterized. This is due, in part, to the antigenic similarity between ZIKV and closely related Dengue virus (DENV) serotypes. Since these and other similar viruses co-circulate and are spread by the same mosquito species, it is difficult to disentangle ZIKV-specific antibody responses from responses to closely-related arboviruses in humans. Here we use high-density peptide microarrays to differentiate ZIKV from DENV antibody reactivity in pregnant and non-pregnant macaque monkeys with known exposure histories. We independently confirm a ZIKV-specific IgG antibody response targeting ZIKV nonstructural protein 2B (NS2B) that was recently reported in ZIKV-infected people and show that antibody reactivity in pregnant animals can be detectable as late as 113 days post-infection (dpi). We also show, however, these responses wane over time, and in one case the response was elicited following DENV infection in a previously ZIKV-exposed animal. The generally weak and short-lived antibody responses to this NS2B epitope, the only reliably ZIKV-specific epitope identified to date to our knowledge, suggest epidemiologic studies assessing seroprevalence specifically to ZIKV using linear epitope-based strategies may be prone to false negative or otherwise confounded results. These results additionally indicate some antibodies produced in response to ZIKV infection are in circulation for only a short period of time.

IMPORTANCE

Infection with ZIKV during pregnancy can lead to congenital ZIKV infection and associated birth defects. The vulnerability of communities to future ZIKV outbreaks will

47 depend, in part, on the prevalence of immunity, which is thought to be mediated
48 principally by antibodies. We currently lack diagnostic assays to differentiate ZIKV-
49 specific antibodies from antibodies directed against closely related DENV and we do not
50 know how long anti-ZIKV responses persist. Here we profile antibodies recognizing
51 linear epitopes throughout the entire ZIKV and DENV polyproteins and show that while
52 ZIKV-specific antibody responses can be detected, these responses are generally weak
53 and ephemeral. This may complicate efforts to identify people previously infected with
54 ZIKV and to determine ZIKV seroprevalence, and it raises questions about the utility of
55 linear epitope-based technologies in defining ZIKV infection history.
56

57 **INTRODUCTION**

58 Zika virus (ZIKV) serologic assays suffer from cross-reactivity with closely related and
59 co-endemic Dengue virus (DENV), due to the high level (average ~55%) of amino acid
60 sequence identity and structural similarity (1-4) of ZIKV and DENV. Serologic assays
61 have been developed to detect past ZIKV infection, reporting sensitivity varying from
62 37% to 97% and specificity varying from 20% to 90% (5-8). Most of these assays have
63 focused on antibodies to the ZIKV envelope protein or nonstructural protein 1 (NS1) (7,
64 9-11). A recent publication by Mishra et al. employed a high-density peptide microarray
65 to identify antibodies to linear ZIKV epitopes that do not cross-react with other
66 flaviviruses (12). This group identified an IgG immunoreactive peptide sequence in ZIKV
67 nonstructural protein 2B (NS2B) which induces little or no antibody binding in serum
68 from ZIKV-naive people or people with history of infection with other flaviviruses (12).
69 This suggests profiling antibody binding against the entire viral proteome may identify

70 unexpected epitopes with useful properties, such as cross-reactivity with multiple similar
71 viruses or specificity to a single virus.
72
73 Because ZIKV, DENV, and other flaviviruses are similar in structure and clinical
74 syndrome, are spread by the same mosquito vectors (13), and are co-endemic (14, 15),
75 it is difficult to identify people who have unequivocally been exposed to ZIKV only,
76 making it difficult to profile ZIKV-specific antibody responses. In contrast, macaques
77 raised in indoor colonies can be infected specifically with ZIKV or DENV. Macaque
78 models of ZIKV infection provide a close approximation of human ZIKV infection in
79 regards to natural history (16-19), tissue tropism (16, 17, 20, 21), and transmission (17,
80 22-25). Importantly, macaques infected with ZIKV during pregnancy provide insight into
81 the pathogenesis of congenital ZIKV infection (17, 18, 21, 22, 26, 27). Since the strain,
82 dose, and timing of ZIKV infection is exactly known, the kinetics and specificity of
83 humoral immune responses can be profiled in macaques with better resolution than is
84 possible in cross-sectional human studies.
85
86 Here, we used high-density peptide microarrays to map macaque IgG epitopes in full-
87 length ZIKV and DENV polyproteins. This peptide microarray technology allows for one
88 serum sample to be assayed against six million unique 16-residue peptides or, as was
89 done in this study, for 12 samples to each be assayed against 392,000 peptides on a
90 single chip (Roche Sequencing Solutions, Madison, WI). This technology has been
91 used in proteome-wide epitope mapping (28), profiling of antibody responses in
92 autoimmune disease (29), profiling venom toxin epitopes (30), determining functions of

93 cellular enzymes (31), *de novo* binding sequence discovery (32), epitope validation
94 following phage display screening (33), and screening for tick-borne disease
95 seroprevalence (34). We previously used this tool to examine antibody responses in
96 simian pegivirus (SPgV) and simian immunodeficiency virus (SIV) infections (35). As
97 mentioned above, a recent publication explored use of this technology in profiling
98 human antibody responses against flaviviruses (12). This linear peptide microarray
99 technology has advantages over previous assays through its capability to screen for
100 reactivity to a large number of pathogens while simultaneously mapping reactive
101 peptides precisely, and it has the distinct advantage of allowing detection of unexpected
102 epitopes due to its capacity to assay the entirety of a virus's proteome.
103

104 **RESULTS**

105 **Ultradense peptide microarray identifies SIV-specific IgG epitopes**

106 To assess the performance of the recently-developed peptide microarray platform we
107 sought to test its performance against a well-characterized immune response. We
108 synthesized 16-mer peptides overlapping by 12 amino acids representing the
109 SIVmac239 envelope protein (env) and analyzed serum from two cynomolgus
110 macaques for SIV-specific IgG reactivity before and approximately 125 days after
111 SIVmac239 infection (Table 1). We previously plotted data from these samples (35);
112 here we show the same data using an updated, improved data processing pipeline that
113 is used throughout this manuscript. Post-infection samples exhibited reactivity as high
114 as 1,000 times the reactivity in pre-infection samples (Figure 1). Regions of higher-fold
115 increases in reactivity corresponded to previously defined variable domains of env

116 which are known antibody targets, the variable loop regions, as well as others
117 corresponding to known epitopes (36). Taken together, these results demonstrate the
118 peptide microarray platform is capable of high resolution virus-specific IgG epitope
119 identification.
120
121 **Identification of ZIKV polyprotein epitopes**
122 Next we sought to determine reactivity to the ZIKV polyprotein following ZIKV infection.
123 We assessed reactivity against ZIKV polyproteins represented by 16-mer peptides
124 (overlapping by 15 amino acids) of serum from animals with recent ZIKV-FP (animals
125 B1, D1, and D2) or ZIKV-MR766 (animal C1) infections (Table 1). Animals in both
126 groups demonstrated neutralizing antibody responses at 28 dpi, measured by 90%
127 plaque reduction neutralization tests ($PRNT_{90}$) as described previously (16, 23, 37).
128 Peptides were defined as reactive if the normalized signal intensity was greater after
129 infection with a cognate strain (e.g., increased signal intensity against ZIKV peptides in
130 an animal infected with ZIKV) than it was before infection. Peptides were defined as
131 cross-reactive if the normalized signal intensity was greater after infection with a
132 noncognate strain (e.g., increased signal intensity against ZIKV peptides in an animal
133 infected with DENV). In regions of interest, such as the epitope in NS2B in which a
134 ZIKV-specific epitope was identified, statistical significance of the change in signal
135 intensity versus no change was calculated using a two-tailed log-ratio t-test. Given the
136 small offset between adjacent peptides, true epitopes were expected to induce antibody
137 binding to multiple peptides with overlapping sequences; thus regions were only

138 considered epitopic when there was a statistically significant increase in post-infection
139 reactivity relative to pre-infection reactivity in three or more consecutive peptides.
140
141 Reactivity was most commonly observed in three regions: envelope protein, NS2B, and
142 nonstructural protein 3 (NS3). Antibody responses against the envelope protein were
143 seen in four out of four animals at 28 dpi; responses against nonstructural protein NS3
144 (NS3) were seen in three out of four (Figure 2). All four animals exhibited an antibody
145 response to the ZIKV NS2B epitope similar to that documented in humans (12). Area
146 under the curve (AUC) values and corresponding receiver operating characteristic
147 (ROC) curves were calculated (supplemental figure S1), identifying ten peptides at
148 positions 1427-1436 in the polyprotein (for a total of 25 amino acids, sequence
149 RAGDITWEKDAEVTGNSPRLDVALD) as the best-performing epitope, hereafter
150 referred to as $NS2B_{1427-1451}$RD25 (AUC of 0.9375, 95% confidence interval of 0.89065
151 to 0.9375). This epitope is slightly larger in size than that found by Mishra et al. (nine
152 12-mer peptides, for a total of 20 amino acids, sequence DITWEKDAEVTGNSPRLDVA)
153 (12). The four animals exhibited similar responses against an Asian ZIKV strain, ZIKV-
154 FP (Figure 2), as against an African strain and an American strain (ZIKV-MR766 and
155 ZIKV-PR respectively, supplemental figure S2). Animals infected with either of the ZIKV-
156 FP or ZIKV-MR766 strains showed similar reactivity against the ZIKV polyprotein
157 (supplemental figure S3).
158
159 **Cross-reactivity of ZIKV-convalescent serum with DENV polyproteins**

160 DENV polyproteins share an average of 55% sequence identity with ZIKV polyproteins
161 (1, 2), and the DENV NS2B region corresponding to the immunoreactive ZIKV
162 NS2B$_{1427-1451}$RD25 shares an average of 41% identity (Figure 3 A). To examine cross-
163 reactivity, we analyzed the antibody responses of the ZIKV-convalescent animals to
164 DENV polyproteins represented on the array (Figure 3 B-E). Cross-reactivity was
165 apparent, with antibodies from the ZIKV-convalescent but DENV-naive animals
166 recognizing regions of DENV polyproteins. All four animals showed only minimal
167 reactivity against DENV envelope protein and DENV NS3. Animals exhibited
168 comparable cross-reactivities to all four DENV serotypes, with the highest single
169 instance of cross-reactivity observed against a DENV-3 epitope in the NS3 region. No
170 significant cross-reactivity against the DENV NS2B protein was observed.
171

172 **Differentiating DENV from ZIKV serologic responses**

173 Previous assays have struggled to distinguish DENV serologic responses from ZIKV
174 serologic responses (5-8). We investigated whether reactivity against the peptide
175 microarray and specifically against the ZIKV NS2B$_{1427-1451}$RD25 epitope could
176 distinguish a recent DENV infection in an animal with previous ZIKV exposure. Three
177 animals (cohort F) had been challenged twice with ZIKV-FP 12 months prior and 9.5
178 months prior (16); we infected these animals with DENV-2 and collected serum samples
179 prior to DENV-2 infection and 28 days after. These samples were analyzed against 16-
180 mer peptides, with amino acid overlap of 12, representing ZIKV-FP (Figure 4).
181

182 These animals showed reactivity against all four DENV polyproteins in regions
183 representing the DENV envelope protein, DENV NS3, and others (supplemental figure
184 S4) and cross-reactivity against corresponding regions of the ZIKV polyprotein (Figure
185 4). One animal (F3) showed reactivity to the NS2B$_{1427\text{-}1451}$RD25 epitope, though this
186 reactivity was slightly outside the area of typical NS2B$_{1427\text{-}1451}$RD25 reactivity (peptides
187 1421-1429 rather than 1427-1436).
188
189 **Anti-ZIKV antibody response during pregnancy**
190 Given the importance of determining an accurate ZIKV infection history in pregnancy,
191 we sought to characterize the gestational anti-ZIKV antibody response. We used the
192 peptide microarray to evaluate serum samples from six pregnant animals. Animals were
193 inoculated with ZIKV at 35-47 days post-conception (gestational date, gd) (Table 2).
194 Two animals (G1 and G2) had no history of flavivirus exposure and were inoculated with
195 ZIKV-FP at 36-38 gd. Three more flavivirus-naive animals (H1, H2, and H3) were
196 infected with ZIKV-PR at 45-47 gd. One animal (I1) had a history of exposure to DENV-
197 3 nine months prior to inoculation with a barcoded clone of ZIKV-PR at 35 dpi (38).
198
199 Serum samples collected approximately one week post-infection and at two to six week
200 intervals thereafter were analyzed against flavivirus polyproteins represented on the
201 peptide array (Figure 5). All six pregnant animals exhibited anti-NS2B$_{1427\text{-}1451}$RD25
202 reactivity by the early convalescent phase (21-29 dpi), though time of initial appearance
203 and duration of the response varied between animals.
204

205 In G1, elevated baseline intensity in the ZIKV NS2B$_{1427-1451}$RD25 region was present
206 prior to inoculation with ZIKV-FP. This animal experienced one of the highest levels of
207 anti-ZIKV IgG reactivity in this study (magnitude of fluorescence intensity reaching
208 6338.7 AU, or 13.1 on the log base 2 scale) in the acute phase (7 dpi). Reactivity
209 subsequently decreased but remained above pre-infection levels through 78 dpi. The
210 anti-NS2B$_{1427-1451}$RD25 intensity level fell below the pre-infection level by 127 dpi, after
211 G1 had given birth. In G2, reactivity was not appreciable until the early convalescent
212 phase (21 dpi) but remained above pre-infection levels until the latest time point
213 analyzed (113 dpi).
214
215 Both H1 and H2 showed reactivity against NS2B$_{1427-1451}$RD25 during acute infection (7
216 dpi) and all three animals in cohort H showed reactivity by the early convalescent phase
217 (21 dpi). This reactivity decreased to or below pre-infection levels for H1 and H3 but not
218 H2 by 70 dpi.
219
220 I1, an animal nine months post-DENV-3 infection, showed a pattern of reactivity similar
221 to the other animals, with anti-NS2B$_{1427-1451}$RD25 IgG reactivity first appearing at 8 dpi
222 and peaking at 29 dpi at a level 9 times pre-infection reactivity (Figure 5 F). I1 was the
223 only animal in this study for which reactivity remained close to peak reactivity by 78 dpi.
224
225 All pregnant animals' cross-reactivity against DENV polyproteins mirrored that in non-
226 pregnant animals (supplemental figure S6). All animals in which fluorescence intensity
227 at the NS2B$_{1427-1451}$RD25 epitope was higher at pre-infection time points than at post-

228 infection time points had this effect only for the NS2B$_{1427-1451}$RD25 epitope and not for
229 other immunoreactive regions of the ZIKV polyprotein (supplemental figure S5).
230
231 **Kinetics of anti-ZIKV IgG responses**
232 The duration of antibody responses following ZIKV infection has not yet been
233 established. Our data provide preliminary insight into the strength and duration of anti-
234 ZIKV antibody responses.
235
236 Kinetics of IgG binding at the NS2B$_{1427-1451}$RD25 epitope were followed during the
237 course of infection using fold change from pre-infection levels. Non-pregnant animals
238 (B1, C1, D1, and D2) exhibited a characteristic rise and fall in reactivity, with greatest
239 fold increase consistently noted at early convalescence, 28 dpi (supplemental figure S7
240 A). At 28 dpi B1 and C1 exhibited a 5.7-fold reactivity increase above pre-infection
241 levels; by 67 dpi these levels had fallen to 3.1-fold and 5.5-fold respectively,
242 representing a 46% decrease and a 4% decrease in anti-NS2B$_{1427-1451}$RD25 reactivity in
243 39 days. Animals D1 and D2 showed reactivity increased 2.4-fold and 1.2-fold above
244 pre-infection levels at 28 dpi. Likewise, samples from D1 and D2 in late convalescence
245 (621 and 582 dpi, respectively) showed a decline in IgG reactivity (to 0.92-fold and 0.82-
246 fold, respectively).
247
248 Kinetics in pregnant animals were tracked more extensively (supplemental figure S7 B).
249 One animal, G1, exhibited unusually high pre-infection fluorescence intensity (to a
250 normalized level of 10.2; see Figure 5) at the NS2B$_{1427-1451}$RD25 epitope prior to

251 infection; G1's reactivity peaked from 7 to 21 dpi at a 2.3-fold increase over pre-infection
252 levels. Reactivity decreased by 78 dpi and fell 4.6-fold below pre-infection levels by 127
253 dpi. Animal G2 first demonstrated reactivity at 21 dpi, reaching peak reactivity at 78 dpi
254 and falling thereafter, with levels still above pre-infection through the latest time
255 examined (113 dpi). Two animals in cohort H, H1 and H3, showed ZIKV-specific
256 reactivity at 7 dpi, and H3 reached peak reactivity at this time. H1 and H2 exhibited
257 peak reactivity at 21 dpi, and reactivity in animals H1 and H3 had returned to or fallen
258 below pre-infection levels by 70 dpi. Animal I1, with history of previous DENV-3
259 infection, first showed NS2B$_{1427\text{-}1451}$RD25 reactivity at 8 dpi with peak reactivity at 29
260 dpi, with reactivity remaining close to peak reactivity through the last day examined, 78
261 dpi.
262
263 **DISCUSSION**
264 We describe the anti-ZIKV IgG response in non-pregnant and pregnant rhesus
265 macaques and compare this to the anti-DENV response. Using a recently developed
266 high-density peptide microarray we show macaques infected with ZIKV produce IgG
267 antibodies reactive against the ZIKV polyprotein, including a conserved response
268 against an epitope in ZIKV NS2B, NS2B$_{1427\text{-}1451}$RD25, that is apparent regardless of the
269 ZIKV strain used for infection. We establish cross-reactivity between anti-ZIKV and anti-
270 DENV antibodies for the ZIKV and DENV polyproteins. Additionally we show the anti-
271 NS2B$_{1427\text{-}1451}$RD25 IgG response in ZIKV, an acute infection, is low in magnitude and
272 brief in duration compared to the antibody reactivity induced by SIV, a chronic infection.
273

274 As seen in previous assays (2, 12, 39-41), we observed antibody cross-reactivity
275 between ZIKV- and DENV-immune serum, though reactivity to the ZIKV NS2B$_{1427-}$
276 $_{1451}$RD25 epitope was observed in all cases of recent ZIKV infection (12 out of 12 ZIKV-
277 infected animals) and in only one out of three instances of recent DENV infection.
278 Inoculation with African, Asian, and American ZIKV strains induced some variability in
279 responses, though reactivity to the NS2B epitope was conserved throughout. All ZIKV-
280 infected animals produced anti-ZIKV IgG against the NS2B$_{1427-1451}$RD25 epitope, though
281 reactivity was sometimes only slightly above an animal's pre-infection baseline (as in
282 animal D2) or was measurable for only a short duration (as in animal H3). The lack of
283 uniformity of the anti-ZIKV IgG response is especially relevant since all ZIKV-exposed
284 animals could be followed, in contrast to work in humans where there may be a
285 selection bias for individuals with symptomatic ZIKV, thought to account for only
286 approximately half of ZIKV infections (12, 42). Though anti-NS2B$_{1427-1451}$RD25 reactivity
287 was consistently present in early convalescence, it was observed to decay in all but one
288 case during the time period assessed. These findings corroborate findings in humans, in
289 which antibody reactivity in symptomatic patients was strongly associated with a
290 detectable NS2B response in the early convalescent phase (96%), but less likely six
291 months post-infection (44%) (12). These results demonstrate the need for investigation
292 into the longevity and kinetics of the anti-ZIKV antibody response. Given that this is the
293 only linear epitope identified to date as being reliably ZIKV-specific (12), and given that
294 antibodies to this epitope appear to drop to undetectable levels in at least 50% of
295 individuals by six months post-infection, these results also call into question how useful
296 current serological methods may be in differentiating past ZIKV exposure from exposure

297 to other flaviviruses. Additionally, one animal (F3) showed reactivity against the ZIKV
298 NS2B$_{1427-1451}$RD25 epitope 28 days after DENV infection, possibly as an effect of having
299 been infected with ZIKV 12 and 9.5 months prior. Thus, while the specificity of this
300 epitope is important, its utility in guiding development of diagnostics will likely be limited.
301
302 This array detected anti-NS2B$_{1427-1451}$RD25 reactivity in all pregnant macaques exposed
303 to ZIKV. Production of IgG antibodies has relevance to both mother and fetus, since
304 maternal IgG crosses the placenta freely and maternal donation of IgG increases
305 throughout pregnancy (43). It can be assumed the anti-ZIKV IgG produced by these
306 animals also reached their fetuses, but whether these anti-NS2B$_{1427-1451}$RD25
307 antibodies provide protection or whether they contribute to the pathology of ZIKV
308 disease and ZIKV congenital effects is currently unknown. We did not note any variation
309 in outcomes with variation in antibody responses, but it is possible variation in antibody
310 responses during pregnancy could help explain differences in outcomes following
311 gestational ZIKV infection. Several pregnant animals also showed post-infection
312 reactivity against the NS2B$_{1427-1451}$RD25 epitope that was lower than their pre-infection
313 reactivity. It is possible these animals were exposed to some substance similar to the
314 NS2B$_{1427-1451}$RD25 epitope that caused them to produce antibodies against it before
315 exposure to ZIKV, or that there is some genetic characteristic or some aspect of
316 pregnancy that causes increased likelihood of producing anti-NS2B$_{1427-1451}$RD25
317 antibodies prior to ZIKV exposure, though we have not found this epitope present in any
318 other pathogen. These findings merit further and more thorough investigation than this
319 current study can provide.

320

321 The peptide array technology used in this study has several limitations. Utility of the
322 assay will depend upon the magnitude of the antibody response induced, which varies
323 from pathogen to pathogen. In this study the magnitude of antibody reactivity induced
324 by ZIKV infection was markedly lower (165 times lower at peak reactivity) than that
325 induced by SIV infection. Our study defined positive responses as an increase from an
326 animal's pre-infection reactivity; human patients cannot give pre-infection samples and
327 must rely upon on controls determined from humans having no known history of
328 flavivirus exposure (12). We simulated the performance of this assay without the
329 availability of pre-infection samples by defining a positivity threshold using the average
330 reactivity of macaque pre-infection samples + 1 standard deviation; application of this
331 control caused some animals with lower reactivity (D1 and D2) to appear to lose their
332 post-infection positivity. Applying a control using the average of pre-infection samples +
333 2 standard deviations resulted in even more false negatives. Our control was limited by
334 small sample size, but these results raise the possibility of lower sensitivity when
335 definitive pre-infection samples from the same individual are not available.

336

337 The peptide array approach is also limited due to its detection only of continuous linear
338 epitopes. Many documented ZIKV epitopes are conformational discontinuous epitopes
339 (44-49). Other epitope discovery methods will likely remain superior in defining
340 discontinuous epitopes, but peptide microarrays are useful in identifying
341 immunoreactive regions not previously considered as potential epitopes. Past work from
342 our laboratory, including results from some of the animals analyzed here, has shown

343 anti-ZIKV neutralizing antibody titers measured by $PRNT_{90}$ do not drop off but remain
344 elevated as late as 64 dpi (16). The discordance between levels of anti-$NS2B_{1427-}$
345 $_{1451}$RD25 IgG and neutralizing antibody titers may indicate the anti-$NS2B_{1427-1451}$RD25
346 antibodies do not play a role in protection against future infections, and thus their
347 production is discontinued in favor of antibodies which can neutralize ZIKV virions.
348
349 Despite these limitations, this technology could be useful as a screening tool for
350 antibody reactivity to ZIKV and many other pathogens given its enormous throughput.
351 Little is known about the pervasiveness of ZIKV in Africa, though the virus' presence
352 there was established in 1947. To this end, our group has designed a peptide
353 microarray capable of simultaneously assessing twelve samples' antibody responses
354 against every arbovirus strain known to cause human infection in Africa. We plan to use
355 this array to screen pooled samples for evidence of human antibody reactivity to ZIKV
356 and to the hundreds of other viruses represented. This assay could also be used to
357 compare IgM and IgG responses, a currently untapped potential of this technology.
358
359 In summary, this work in macaques demonstrates the capacity of a recently developed
360 peptide microarray to differentiate anti-ZIKV and anti-DENV IgG antibody responses, a
361 distinction which has previously been difficult. Our work shows the anti-$NS2B_{1427-}$
362 $_{1451}$RD25 IgG response is characterized by relatively low-magnitude antibody responses
363 prone to relatively rapid decay, mirroring the events seen in humans. The peptide
364 microarray design used shows particular promise in evaluating serological reactivity
365 specific to ZIKV while simultaneously evaluating for responses against a large number

366 of other similar or dissimilar pathogens. In the future this technology could be expanded
367 for use in screening populations for exposure to ZIKV, DENV, and a multitude of other
368 pathogens.
369

370 **MATERIALS AND METHODS**

371 **Macaque study design**

372 Animal demographics, inoculation strain, dose, and route, serum sample collection
373 timelines, and array design used for each animal are described in Table 1. Gestational
374 details and outcomes for pregnant animals are described in Table 2. Additional details
375 on the study histories of the animals in this study can be found at
376 https://go.wisc.edu/b726s1.
377

378 **Ethics**

379 All monkeys were cared for by the staff at the Wisconsin National Primate Research
380 Center (WNPRC) in accordance with the regulations and guidelines outlined in the
381 Animal Welfare Act and the Guide for the Care and Use of Laboratory Animals and the
382 recommendations of the Weatherall report (https://royalsociety.org/topics-
383 policy/publications/2006/weatherall-report/). Per WNPRC standard operating
384 procedures for animals assigned to protocols involving the experimental inoculation of
385 an infectious pathogen, environmental enhancement included constant visual, auditory,
386 and olfactory contact with conspecifics, the provision of feeding devices which inspire
387 foraging behavior, the provision and rotation of novel manipulanda (e.g., Kong toys,
388 nylabones, etc.), and enclosure furniture (i.e., perches, shelves). Per Animal Welfare

389 Regulations (Title 9, Chapter 1, Subchapter A, Parts 1–4, Section 3.80 Primary
390 enclosures) the animals were housed in a nonhuman primate Group 3 enclosure with at
391 least 4.3 square feet of floor space and at least 30 inches of height. This study was
392 approved by the University of Wisconsin-Madison Graduate School Institutional Animal
393 Care and Use Committee (animal protocol numbers G005401 and G005443).
394
395 **Virus stocks**
396 SIVmac239 (GenBank accession: M33262) stock was prepared by WNPRC Virology
397 Services. Vero cells were transfected with the SIVmac239 plasmid. Infectious
398 supernatant was then transferred onto rhesus PBMC. The stock was not passaged
399 before collecting and freezing. ZIKV strain H/PF/2013 (GenBank accession: KJ776791)
400 was obtained from Xavier de Lamballerie (European Virus Archive, Marseille, France)
401 and passage history is described in Dudley et al. (16). ZIKV strain MR766, ZIKV strain
402 PRVABC59, and DENV-2 strain New Guinea C were generously provided by Brandy
403 Russell (CDC, Ft. Collins, CO). ZIKV strain MR766 passage history has been described
404 in Aliota et al. (37). A molecularly-barcoded version of ZIKV strain PRVABC59 (Zika
405 virus/H.sapiens-tc/PUR/2015/PRVABC59; GenBank accession: KU501215) was
406 constructed as described in Aliota et al. (38). DENV-2 strain New Guinea C (GenBank
407 accession: FJ390389), originally isolated from a human in New Guinea, underwent 17
408 rounds of amplification on cells and/or suckling mice followed by a single round of
409 amplification on C6/36 cells; virus stocks were prepared by inoculation onto a confluent
410 monolayer of C6/36 mosquito cells. DENV-3 strain Sleman/78 was obtained from the
411 NIH; virus stocks were prepared by a single passage on C6/36 cells.

412

413 **Multiple sequence alignment**

414 Full-length ZIKV and DENV polyprotein sequences were extracted from the National
415 Center for Biotechnology Information (NCBI) database into Geneious Pro 9.1.8
416 (Biomatters, Ltd., Auckland, New Zealand). These sequences included the ZIKV and
417 DENV polyprotein sequences described above (see "Virus stocks"), as well as DENV-1
418 strain VR-1254 (Genbank accession: EU848545) and DENV-4 strain VID-V2055
419 (Genbank accession: KF955510). These amino acid sequences were aligned using the
420 Geneious alignment algorithm as implemented in Geneious Pro 9.1.8 using default
421 parameters (global alignment with free end gaps, cost matrix: Blosum62).

422

423 **Peptide array design and synthesis**

424 Viral protein sequences were selected and submitted to Roche Sequencing Solutions
425 (Madison, WI) for development into a peptide microarray as part of an early access
426 program. Sequences included three ZIKV polyproteins (an Asian strain, ZIKV-FP,
427 Genbank accession: KJ776791.2; an African strain, ZIKV-MR766, Genbank accession:
428 KU720415.1; and an American strain, ZIKV-PR, Genbank accession: KU501215.1), four
429 DENV polyproteins (DENV-1, Genbank accession: EU848545.1; DENV-2, Genbank
430 accession: KM204118.1; DENV-3, Genbank accession: M93130.1; and DENV-4,
431 Genbank accession: KF955510.1), and one SIVmac239 env protein (Genbank
432 accession: AAA47637.1), which were used for analyses in this study. Proteins were tiled
433 as non-redundant 16 amino acid peptides, overlapping by 12 or 15 amino acids. The
434 array designs are publicly available at https://go.wisc.edu/b726s1.

435

436 The peptide sequences were synthesized *in situ* with a Roche Sequencing Solutions
437 Maskless Array Synthesizer (MAS) by light-directed solid-phase peptide synthesis using
438 an amino-functionalized support (Geiner Bio-One) coupled with a 6-aminohexanoic acid
439 linker and amino acid derivatives carrying a photosensitive 2-(2-nitrophenyl)
440 propyloxycarbonyl (NPPOC) protection group (Orgentis Chemicals). Unique peptides
441 were printed in random positions on the array to minimize impact of positional bias.

442

443 **Peptide array sample binding**

444 Macaque serum samples were diluted 1:100 in binding buffer (0.01M Tris-Cl, pH 7.4,
445 1% alkali-soluble casein, 0.05% Tween-20). Diluted sample aliquots and binding buffer-
446 only negative controls were bound to arrays overnight for 16-20 h at 4°C. After binding,
447 the arrays were washed 3x in wash buffer (1x TBS, 0.05% Tween-20), 10 min per wash.
448 Primary sample binding was detected via 8F1-biotin mouse anti-primate IgG (NIH
449 Nonhuman Primate Reagent Resource) secondary antibody. The secondary antibody
450 was diluted 1:10,000 (final concentration 0.1 ng/µl) in secondary binding buffer (1x TBS,
451 1% alkali-soluble casein, 0.05% Tween-20) and incubated with arrays for 3 h at room
452 temperature, then washed 3x in wash buffer (10 min per wash) and 30 sec in reagent-
453 grade water. The secondary antibody was labeled with Cy5-Streptavidin (GE
454 Healthcare; 5 ng/µl in 0.5x TBS, 1% alkali-soluble casein, 0.05% Tween-20) for 1 h at
455 room temperature, then the array was washed 2x for 1 min in 1x TBS, and washed once
456 for 30 sec in reagent-grade water. Fluorescent signal of the secondary antibody was

457 detected by scanning at 635 nm at 2 μm resolution and 25% gain, using an MS200
458 microarray scanner (Roche NimbleGen).
459
460 **Peptide array data processing**
461 The datafiles and analysis code for figures is available from https://go.wisc.edu/b726s1.
462 Fluorescence signal intensities were normalized by background subtraction and quantile
463 normalization across samples. All figures use the log base 2 of the resulting intensity
464 values. For each sample, each unique peptide was assayed and processed once; then
465 results from peptides redundant on the chip (i.e. were present in more than one protein
466 represented) were restored to each protein.
467
468 **Acknowledgments**
469 We would like to thank Adam Ericsen for helpful discussions.
470 Grant support: National Institutes of Health grants R01AI116382 and R24OD017850
471 (ASH, AKH, CRB, AB, DMD, CMN, MK, MEB, MR, LMS, DHO).
472
473 **Conflict of interest**
474 This manuscript describes the use of a platform provided on an early-access basis by
475 Roche Sequencing Solutions. While scientists from Roche were involved in the
476 experimental design and data analysis, the manuscript was prepared independently
477 from Roche and did not require pre-approval from Roche prior to submission. RSP, EB,
478 HL, JP, and JCT are employed by Roche Sequencing Solutions.
479

480 **Supplemental materials**

481 **Supplemental figure S1**: ROC curves for best-performing epitope and

482 multidimensional scaling (MDS) plot for different time points.

483 **Supplemental figure S2**: Reactivity of B1, C1, D1, and D2 against ZIKV-MR766 and

484 ZIKV-PR.

485 **Supplemental figure S3**: Reactivity of B1, C1, D1, and D2 against the complete

486 polyprotein of ZIKV-FP.

487 **Supplemental figure S4**: Reactivity of cohort F against the DENV-2 polyprotein.

488 **Supplemental figure S5**: Reactivity of cohort G, cohort H, and cohort I against the

489 ZIKV-FP polyprotein.

490 **Supplemental figure S6**: Reactivity of cohort G, cohort H, and cohort I against the

491 DENV-2 polyprotein.

492 **Supplemental figure S7**: Kinetics of IgG antibody reactivity against the ZIKV NS2B$_{1427-}$

493 $_{1451}$RD25 epitope

494

495 **References**

496 1. Chang, H. H., Huber, R. G., Bond, P. J., Grad, Y. H., Camerini, D., Maurer-Stroh,

497 S., & Lipsitch, M. (2017). Systematic analysis of protein identity between Zika

498 virus and other arthropod-borne viruses. *Bull World Health Organ, 95*(7), 517-

499 525I. doi:10.2471/BLT.16.182105

500 2. Xu, X., Vaughan, K., Weiskopf, D., Grifoni, A., Diamond, M. S., Sette, A., &

501 Peters, B. (2016). Identifying Candidate Targets of Immune Responses in Zika

502 Virus Based on Homology to Epitopes in Other Flavivirus Species. *PLoS Curr, 8*.
503 doi:10.1371/currents.outbreaks.9aa2e1fb61b0f632f58a098773008c4b
504 3. Xu, X., Song, H., Qi, J., Liu, Y., Wang, H., Su, C., Shi, Y., & Gao, G. F. (2016).
505 Contribution of intertwined loop to membrane association revealed by Zika virus
506 full-length NS1 structure. *EMBO J, 35*(20), 2170-2178.
507 doi:10.15252/embj.201695290
508 4. Harrison, S. C. (2016). Immunogenic cross-talk between dengue and Zika
509 viruses. *Nat Immunol, 17*(9), 1010-1012. doi:10.1038/ni.3539
510 5. Safronetz, D., Sloan, A., Stein, D. R., Mendoza, E., Barairo, N., Ranadheera, C.,
511 Scharikow, L., Holloway, K., Robinson, A., Traykova-Andonova, M., Makowski,
512 K., Dimitrova, K., Giles, E., Hiebert, J., Mogk, R., Beddome, S., & Drebot, M.
513 (2017). Evaluation of 5 Commercially Available Zika Virus Immunoassays. *Emerg*
514 *Infect Dis, 23*(9), 1577-1580. doi:10.3201/eid2309.162043
515 6. Wong, S. J., Furuya, A., Zou, J., Xie, X., Dupuis, A. P., 2nd, Kramer, L. D., & Shi,
516 P. Y. (2017). A Multiplex Microsphere Immunoassay for Zika Virus Diagnosis.
517 *EBioMedicine, 16*, 136-140. doi:10.1016/j.ebiom.2017.01.008
518 7. Granger, D., Hilgart, H., Misner, L., Christensen, J., Bistodeau, S., Palm, J.,
519 Strain, A. K., Konstantinovski, M., Liu, D., Tran, A., & Theel, E. S. (2017).
520 Serologic Testing for Zika Virus: Comparison of Three Zika Virus IgM-Screening
521 Enzyme-Linked Immunosorbent Assays and Initial Laboratory Experiences. *J*
522 *Clin Microbiol, 55*(7), 2127-2136. doi:10.1128/JCM.00580-17
523 8. Goncalves, A., Peeling, R. W., Chu, M. C., Gubler, D. J., de Silva, A. M., Harris,
524 E., Murtagh, M., Chua, A., Rodriguez, W., Kelly, C., & Wilder-Smith, A. (2018).

525 Innovative and New Approaches to Laboratory Diagnosis of Zika and Dengue: A
526 Meeting Report. *J Infect Dis, 217*(7), 1060-1068. doi:10.1093/infdis/jix678
527 9. Lee, A. J., Bhattacharya, R., Scheuermann, R. H., & Pickett, B. E. (2017).
528 Identification of diagnostic peptide regions that distinguish Zika virus from related
529 mosquito-borne Flaviviruses. *PLoS One, 12*(5), e0178199.
530 doi:10.1371/journal.pone.0178199
531 10. Balmaseda, A., Stettler, K., Medialdea-Carrera, R., Collado, D., Jin, X.,
532 Zambrana, J. V., Jaconi, S., Cameroni, E., Saborio, S., Rovida, F., Percivalle, E.,
533 Ijaz, S., Dicks, S., Ushiro-Lumb, I., Barzon, L., Siqueira, P., Brown, D. W. G.,
534 Baldanti, F., Tedder, R., Zambon, M., de Filippis, A. M. B., Harris, E., & Corti, D.
535 (2017). Antibody-based assay discriminates Zika virus infection from other
536 flaviviruses. *Proc Natl Acad Sci U S A, 114*(31), 8384-8389.
537 doi:10.1073/pnas.1704984114
538 11. L'Huillier, A. G., Hamid-Allie, A., Kristjanson, E., Papageorgiou, L., Hung, S.,
539 Wong, C. F., Stein, D. R., Olsha, R., Goneau, L. W., Dimitrova, K., Drebot, M.,
540 Safronetz, D., & Gubbay, J. B. (2017). Evaluation of Euroimmun Anti-Zika Virus
541 IgM and IgG Enzyme-Linked Immunosorbent Assays for Zika Virus Serologic
542 Testing. *J Clin Microbiol, 55*(8), 2462-2471. doi:10.1128/JCM.00442-17
543 12. Mishra, N., Caciula, A., Price, A., Thakkar, R., Ng, J., Chauhan, L. V., Jain, K.,
544 Che, X., Espinosa, D. A., Montoya Cruz, M., Balmaseda, A., Sullivan, E. H.,
545 Patel, J. J., Jarman, R. G., Rakeman, J. L., Egan, C. T., Reusken, C.,
546 Koopmans, M. P. G., Harris, E., Tokarz, R., Briese, T., & Lipkin, W. I. (2018).

547 Diagnosis of Zika Virus Infection by Peptide Array and Enzyme-Linked
548 Immunosorbent Assay. *MBio, 9*(2). doi:10.1128/mBio.00095-18
549 13. Paixao, E. S., Teixeira, M. G., & Rodrigues, L. C. (2018). Zika, chikungunya and
550 dengue: the causes and threats of new and re-emerging arboviral diseases. *BMJ*
551 *Glob Health, 3*(Suppl 1), e000530. doi:10.1136/bmjgh-2017-000530
552 14. Carrillo-Hernandez, M. Y., Ruiz-Saenz, J., Villamizar, L. J., Gomez-Rangel, S. Y.,
553 & Martinez-Gutierrez, M. (2018). Co-circulation and simultaneous co-infection of
554 dengue, chikungunya, and zika viruses in patients with febrile syndrome at the
555 Colombian-Venezuelan border. *BMC Infect Dis, 18*(1), 61. doi:10.1186/s12879-
556 018-2976-1
557 15. Azeredo, E. L., Dos Santos, F. B., Barbosa, L. S., Souza, T. M. A., Badolato-
558 Correa, J., Sanchez-Arcila, J. C., Nunes, P. C. G., de-Oliveira-Pinto, L. M., de
559 Filippis, A. M., Dal Fabbro, M., Hoscher Romanholi, I., & Venancio da Cunha, R.
560 (2018). Clinical and Laboratory Profile of Zika and Dengue Infected Patients:
561 Lessons Learned From the Co-circulation of Dengue, Zika and Chikungunya in
562 Brazil. *PLoS Curr, 10*.
563 doi:10.1371/currents.outbreaks.0bf6aeb4d30824de63c4d5d745b217f5
564 16. Dudley, D. M., Aliota, M. T., Mohr, E. L., Weiler, A. M., Lehrer-Brey, G.,
565 Weisgrau, K. L., Mohns, M. S., Breitbach, M. E., Rasheed, M. N., Newman, C.
566 M., Gellerup, D. D., Moncla, L. H., Post, J., Schultz-Darken, N., Schotzko, M. L.,
567 Hayes, J. M., Eudailey, J. A., Moody, M. A., Permar, S. R., O'Connor, S. L.,
568 Rakasz, E. G., Simmons, H. A., Capuano, S., Golos, T. G., Osorio, J. E.,

569 Friedrich, T. C., & O'Connor, D. H. (2016). A rhesus macaque model of Asian-
570 lineage Zika virus infection. *Nat Commun, 7*, 12204. doi:10.1038/ncomms12204
571 17. Nguyen, S. M., Antony, K. M., Dudley, D. M., Kohn, S., Simmons, H. A., Wolfe,
572 B., Salamat, M. S., Teixeira, L. B. C., Wiepz, G. J., Thoong, T. H., Aliota, M. T.,
573 Weiler, A. M., Barry, G. L., Weisgrau, K. L., Vosler, L. J., Mohns, M. S.,
574 Breitbach, M. E., Stewart, L. M., Rasheed, M. N., Newman, C. M., Graham, M.
575 E., Wieben, O. E., Turski, P. A., Johnson, K. M., Post, J., Hayes, J. M., Schultz-
576 Darken, N., Schotzko, M. L., Eudailey, J. A., Permar, S. R., Rakasz, E. G., Mohr,
577 E. L., Capuano, S., 3rd, Tarantal, A. F., Osorio, J. E., O'Connor, S. L., Friedrich,
578 T. C., O'Connor, D. H., & Golos, T. G. (2017). Highly efficient maternal-fetal Zika
579 virus transmission in pregnant rhesus macaques. *PLoS Pathog, 13*(5),
580 e1006378. doi:10.1371/journal.ppat.1006378
581 18. Martinot, A. J., Abbink, P., Afacan, O., Prohl, A. K., Bronson, R., Hecht, J. L.,
582 Borducchi, E. N., Larocca, R. A., Peterson, R. L., Rinaldi, W., Ferguson, M.,
583 Didier, P. J., Weiss, D., Lewis, M. G., De La Barrera, R. A., Yang, E., Warfield, S.
584 K., & Barouch, D. H. (2018). Fetal Neuropathology in Zika Virus-Infected
585 Pregnant Female Rhesus Monkeys. *Cell, 173*(5), 1111-1122 e1110.
586 doi:10.1016/j.cell.2018.03.019
587 19. Osuna, C. E., Lim, S. Y., Deleage, C., Griffin, B. D., Stein, D., Schroeder, L. T.,
588 Omange, R. W., Best, K., Luo, M., Hraber, P. T., Andersen-Elyard, H., Ojeda, E.
589 F., Huang, S., Vanlandingham, D. L., Higgs, S., Perelson, A. S., Estes, J. D.,
590 Safronetz, D., Lewis, M. G., & Whitney, J. B. (2016). Zika viral dynamics and

591 shedding in rhesus and cynomolgus macaques. *Nat Med, 22*(12), 1448-1455.
592 doi:10.1038/nm.4206
593 20. Hirsch, A. J., Smith, J. L., Haese, N. N., Broeckel, R. M., Parkins, C. J.,
594 Kreklywich, C., DeFilippis, V. R., Denton, M., Smith, P. P., Messer, W. B., Colgin,
595 L. M., Ducore, R. M., Grigsby, P. L., Hennebold, J. D., Swanson, T., Legasse, A.
596 W., Axthelm, M. K., MacAllister, R., Wiley, C. A., Nelson, J. A., & Streblow, D. N.
597 (2017). Zika Virus infection of rhesus macaques leads to viral persistence in
598 multiple tissues. *PLoS Pathog, 13*(3), e1006219.
599 doi:10.1371/journal.ppat.1006219
600 21. Hirsch, A. J., Roberts, V. H. J., Grigsby, P. L., Haese, N., Schabel, M. C., Wang,
601 X., Lo, J. O., Liu, Z., Kroenke, C. D., Smith, J. L., Kelleher, M., Broeckel, R.,
602 Kreklywich, C. N., Parkins, C. J., Denton, M., Smith, P., DeFilippis, V., Messer,
603 W., Nelson, J. A., Hennebold, J. D., Grafe, M., Colgin, L., Lewis, A., Ducore, R.,
604 Swanson, T., Legasse, A. W., Axthelm, M. K., MacAllister, R., Moses, A. V.,
605 Morgan, T. K., Frias, A. E., & Streblow, D. N. (2018). Zika virus infection in
606 pregnant rhesus macaques causes placental dysfunction and immunopathology.
607 *Nat Commun, 9*(1), 263. doi:10.1038/s41467-017-02499-9
608 22. Mohr, E. L., Block, L. N., Newman, C. M., Stewart, L. M., Koenig, M., Semler, M.,
609 Breitbach, M. E., Teixeira, L. B. C., Zeng, X., Weiler, A. M., Barry, G. L., Thoong,
610 T. H., Wiepz, G. J., Dudley, D. M., Simmons, H. A., Mejia, A., Morgan, T. K.,
611 Salamat, M. S., Kohn, S., Antony, K. M., Aliota, M. T., Mohns, M. S., Hayes, J.
612 M., Schultz-Darken, N., Schotzko, M. L., Peterson, E., Capuano, S., 3rd, Osorio,
613 J. E., O'Connor, S. L., Friedrich, T. C., O'Connor, D. H., & Golos, T. G. (2018).

614 Ocular and uteroplacental pathology in a macaque pregnancy with congenital
615 Zika virus infection. *PLoS One, 13*(1), e0190617.
616 doi:10.1371/journal.pone.0190617
617 23. Newman, C. M., Dudley, D. M., Aliota, M. T., Weiler, A. M., Barry, G. L., Mohns,
618 M. S., Breitbach, M. E., Stewart, L. M., Buechler, C. R., Graham, M. E., Post, J.,
619 Schultz-Darken, N., Peterson, E., Newton, W., Mohr, E. L., Capuano, S., 3rd,
620 O'Connor, D. H., & Friedrich, T. C. (2017). Oropharyngeal mucosal transmission
621 of Zika virus in rhesus macaques. *Nat Commun, 8*(1), 169. doi:10.1038/s41467-
622 017-00246-8
623 24. Dudley, D. M., Newman, C. M., Lalli, J., Stewart, L. M., Koenig, M. R., Weiler, A.
624 M., Semler, M. R., Barry, G. L., Zarbock, K. R., Mohns, M. S., Breitbach, M. E.,
625 Schultz-Darken, N., Peterson, E., Newton, W., Mohr, E. L., Capuano, S., III,
626 Osorio, J. E., O'Connor, S. L., O'Connor, D. H., Friedrich, T. C., & Aliota, M. T.
627 (2017). Infection via mosquito bite alters Zika virus tissue tropism and replication
628 kinetics in rhesus macaques. *Nat Commun, 8*(1), 2096. doi:10.1038/s41467-017-
629 02222-8
630 25. Haddow, A. D., Nalca, A., Rossi, F. D., Miller, L. J., Wiley, M. R., Perez-Sautu,
631 U., Washington, S. C., Norris, S. L., Wollen-Roberts, S. E., Shamblin, J. D.,
632 Kimmel, A. E., Bloomfield, H. A., Valdez, S. M., Sprague, T. R., Principe, L. M.,
633 Bellanca, S. A., Cinkovich, S. S., Lugo-Roman, L., Cazares, L. H., Pratt, W. D.,
634 Palacios, G. F., Bavari, S., Pitt, M. L., & Nasar, F. (2017). High Infection Rates
635 for Adult Macaques after Intravaginal or Intrarectal Inoculation with Zika Virus.
636 *Emerg Infect Dis, 23*(8), 1274-1281. doi:10.3201/eid2308.170036

637 26. Adams Waldorf, K. M., Stencel-Baerenwald, J. E., Kapur, R. P., Studholme, C.,
638 Boldenow, E., Vornhagen, J., Baldessari, A., Dighe, M. K., Thiel, J., Merillat, S.,
639 Armistead, B., Tisoncik-Go, J., Green, R. R., Davis, M. A., Dewey, E. C.,
640 Fairgrieve, M. R., Gatenby, J. C., Richards, T., Garden, G. A., Diamond, M. S.,
641 Juul, S. E., Grant, R. F., Kuller, L., Shaw, D. W., Ogle, J., Gough, G. M., Lee, W.,
642 English, C., Hevner, R. F., Dobyns, W. B., Gale, M., Jr., & Rajagopal, L. (2016).
643 Fetal brain lesions after subcutaneous inoculation of Zika virus in a pregnant
644 nonhuman primate. *Nat Med, 22*(11), 1256-1259. doi:10.1038/nm.4193
645 27. Adams Waldorf, K. M., Nelson, B. R., Stencel-Baerenwald, J. E., Studholme, C.,
646 Kapur, R. P., Armistead, B., Walker, C. L., Merillat, S., Vornhagen, J., Tisoncik-
647 Go, J., Baldessari, A., Coleman, M., Dighe, M. K., Shaw, D. W. W., Roby, J. A.,
648 Santana-Ufret, V., Boldenow, E., Li, J., Gao, X., Davis, M. A., Swanstrom, J. A.,
649 Jensen, K., Widman, D. G., Baric, R. S., Medwid, J. T., Hanley, K. A., Ogle, J.,
650 Gough, G. M., Lee, W., English, C., Durning, W. M., Thiel, J., Gatenby, C.,
651 Dewey, E. C., Fairgrieve, M. R., Hodge, R. D., Grant, R. F., Kuller, L., Dobyns,
652 W. B., Hevner, R. F., Gale, M., Jr., & Rajagopal, L. (2018). Congenital Zika virus
653 infection as a silent pathology with loss of neurogenic output in the fetal brain.
654 *Nat Med, 24*(3), 368-374. doi:10.1038/nm.4485
655 28. Forsstrom, B., Axnas, B. B., Stengele, K. P., Buhler, J., Albert, T. J., Richmond,
656 T. A., Hu, F. J., Nilsson, P., Hudson, E. P., Rockberg, J., & Uhlen, M. (2014).
657 Proteome-wide epitope mapping of antibodies using ultra-dense peptide arrays.
658 *Mol Cell Proteomics, 13*(6), 1585-1597. doi:10.1074/mcp.M113.033308

659 29. Zandian, A., Forsstrom, B., Haggmark-Manberg, A., Schwenk, J. M., Uhlen, M.,
660 Nilsson, P., & Ayoglu, B. (2017). Whole-Proteome Peptide Microarrays for
661 Profiling Autoantibody Repertoires within Multiple Sclerosis and Narcolepsy. *J*
662 *Proteome Res, 16*(3), 1300-1314. doi:10.1021/acs.jproteome.6b00916
663 30. Engmark, M., Andersen, M. R., Laustsen, A. H., Patel, J., Sullivan, E., de Masi,
664 F., Hansen, C. S., Kringelum, J. V., Lomonte, B., Gutierrez, J. M., & Lund, O.
665 (2016). High-throughput immuno-profiling of mamba (Dendroaspis) venom toxin
666 epitopes using high-density peptide microarrays. *Sci Rep, 6*, 36629.
667 doi:10.1038/srep36629
668 31. Steffen, W., Ko, F. C., Patel, J., Lyamichev, V., Albert, T. J., Benz, J., Rudolph,
669 M. G., Bergmann, F., Streidl, T., Kratzsch, P., Boenitz-Dulat, M., Oelschlaegel,
670 T., & Schraeml, M. (2017). Discovery of a microbial transglutaminase enabling
671 highly site-specific labeling of proteins. *J Biol Chem, 292*(38), 15622-15635.
672 doi:10.1074/jbc.M117.797811
673 32. Lyamichev, V. I., Goodrich, L. E., Sullivan, E. H., Bannen, R. M., Benz, J., Albert,
674 T. J., & Patel, J. J. (2017). Stepwise Evolution Improves Identification of Diverse
675 Peptides Binding to a Protein Target. *Sci Rep, 7*(1), 12116. doi:10.1038/s41598-
676 017-12440-1
677 33. Christiansen, A., Kringelum, J. V., Hansen, C. S., Bogh, K. L., Sullivan, E., Patel,
678 J., Rigby, N. M., Eiwegger, T., Szepfalusi, Z., de Masi, F., Nielsen, M., Lund, O.,
679 & Dufva, M. (2015). High-throughput sequencing enhanced phage display
680 enables the identification of patient-specific epitope motifs in serum. *Sci Rep, 5*,
681 12913. doi:10.1038/srep12913

682 34. Tokarz, R., Mishra, N., Tagliafierro, T., Sameroff, S., Caciula, A., Chauhan, L.,
683 Patel, J., Sullivan, E., Gucwa, A., Fallon, B., Golightly, M., Molins, C., Schriefer,
684 M., Marques, A., Briese, T., & Lipkin, W. I. (2018). A multiplex serologic platform
685 for diagnosis of tick-borne diseases. *Sci Rep, 8*(1), 3158. doi:10.1038/s41598-
686 018-21349-2
687 35. Bailey, A. L., Buechler, C. R., Matson, D. R., Peterson, E. J., Brunner, K. G.,
688 Mohns, M. S., Breitbach, M., Stewart, L. M., Ericsen, A. J., Newman, C. M.,
689 Koenig, M. R., Mohr, E., Tan, J., Capuano, S., 3rd, Simmons, H. A., Yang, D. T.,
690 & O'Connor, D. H. (2017). Pegivirus avoids immune recognition but does not
691 attenuate acute-phase disease in a macaque model of HIV infection. *PLoS*
692 *Pathog, 13*(10), e1006692. doi:10.1371/journal.ppat.1006692
693 36. Pahar, B., Kenway-Lynch, C. S., Marx, P., Srivastav, S. K., LaBranche, C.,
694 Montefiori, D. C., & Das, A. (2016). Breadth and magnitude of antigen-specific
695 antibody responses in the control of plasma viremia in simian immunodeficiency
696 virus infected macaques. *Virol J, 13*(1), 200. doi:10.1186/s12985-016-0652-x
697 37. Aliota, M. T., Dudley, D. M., Newman, C. M., Mohr, E. L., Gellerup, D. D.,
698 Breitbach, M. E., Buechler, C. R., Rasheed, M. N., Mohns, M. S., Weiler, A. M.,
699 Barry, G. L., Weisgrau, K. L., Eudailey, J. A., Rakasz, E. G., Vosler, L. J., Post,
700 J., Capuano, S., 3rd, Golos, T. G., Permar, S. R., Osorio, J. E., Friedrich, T. C.,
701 O'Connor, S. L., & O'Connor, D. H. (2016). Heterologous Protection against
702 Asian Zika Virus Challenge in Rhesus Macaques. *PLoS Negl Trop Dis, 10*(12),
703 e0005168. doi:10.1371/journal.pntd.0005168

704 38. Aliota, M. T., Dudley, D. M., Newman, C. M., Weger-Lucarelli, J., Stewart, L. M.,
705 Koenig, M. R., Breitbach, M. E., Weiler, A. M., Semler, M. R., Barry, G. L.,
706 Zarbock, K. R., Haj, A. K., Moriarty, R. V., Mohns, M. S., Mohr, E. L., Venturi, V.,
707 Schultz-Darken, N., Peterson, E., Newton, W., Schotzko, M. L., Simmons, H. A.,
708 Mejia, A., Hayes, J. M., Capuano, S., 3rd, Davenport, M. P., Friedrich, T. C.,
709 Ebel, G. D., O'Connor, S. L., & O'Connor, D. H. (2018). Molecularly barcoded
710 Zika virus libraries to probe in vivo evolutionary dynamics. *PLoS Pathog, 14*(3),
711 e1006964. doi:10.1371/journal.ppat.1006964
712 39. Lindsey, N. P., Staples, J. E., Powell, K., Rabe, I. B., Fischer, M., Powers, A. M.,
713 Kosoy, O. I., Mossel, E. C., Munoz-Jordan, J. L., Beltran, M., Hancock, W. T.,
714 Toews, K. E., Ellis, E. M., Ellis, B. R., Panella, A. J., Basile, A. J., Calvert, A. E.,
715 Laven, J., Goodman, C. H., Gould, C. V., Martin, S. W., Thomas, J. D.,
716 Villanueva, J., Mataia, M. L., Sciulli, R., Gose, R., Whelen, A. C., & Hills, S. L.
717 (2018). Ability To Serologically Confirm Recent Zika Virus Infection in Areas with
718 Varying Past Incidence of Dengue Virus Infection in the United States and U.S.
719 Territories in 2016. *J Clin Microbiol, 56*(1). doi:10.1128/JCM.01115-17
720 40. Tsai, W. Y., Youn, H. H., Brites, C., Tsai, J. J., Tyson, J., Pedroso, C., Drexler, J.
721 F., Stone, M., Simmons, G., Busch, M. P., Lanteri, M., Stramer, S. L.,
722 Balmaseda, A., Harris, E., & Wang, W. K. (2017). Distinguishing Secondary
723 Dengue Virus Infection From Zika Virus Infection With Previous Dengue by a
724 Combination of 3 Simple Serological Tests. *Clin Infect Dis, 65*(11), 1829-1836.
725 doi:10.1093/cid/cix672

726 41. Ronnberg, B., Gustafsson, A., Vapalahti, O., Emmerich, P., Lundkvist, A.,
727 Schmidt-Chanasit, J., & Blomberg, J. (2017). Compensating for cross-reactions
728 using avidity and computation in a suspension multiplex immunoassay for
729 serotyping of Zika versus other flavivirus infections. *Med Microbiol Immunol,*
730 *206*(5), 383-401. doi:10.1007/s00430-017-0517-y
731 42. Subissi, L., Daudens-Vaysse, E., Cassadou, S., Ledrans, M., Bompard, P.,
732 Gustave, J., Aubry, M., Cao-Lormeau, V. M., & Mallet, H. P. (2017). Revising
733 rates of asymptomatic Zika virus infection based on sentinel surveillance data
734 from French Overseas Territories. *Int J Infect Dis, 65*, 116-118.
735 doi:10.1016/j.ijid.2017.10.009
736 43. Palmeira, P., Quinello, C., Silveira-Lessa, A. L., Zago, C. A., & Carneiro-
737 Sampaio, M. (2012). IgG placental transfer in healthy and pathological
738 pregnancies. *Clin Dev Immunol, 2012*, 985646. doi:10.1155/2012/985646
739 44. Dai, L., Song, J., Lu, X., Deng, Y. Q., Musyoki, A. M., Cheng, H., Zhang, Y.,
740 Yuan, Y., Song, H., Haywood, J., Xiao, H., Yan, J., Shi, Y., Qin, C. F., Qi, J., &
741 Gao, G. F. (2016). Structures of the Zika Virus Envelope Protein and Its Complex
742 with a Flavivirus Broadly Protective Antibody. *Cell Host Microbe, 19*(5), 696-704.
743 doi:10.1016/j.chom.2016.04.013
744 45. Barba-Spaeth, G., Dejnirattisai, W., Rouvinski, A., Vaney, M. C., Medits, I.,
745 Sharma, A., Simon-Loriere, E., Sakuntabhai, A., Cao-Lormeau, V. M., Haouz, A.,
746 England, P., Stiasny, K., Mongkolsapaya, J., Heinz, F. X., Screaton, G. R., &
747 Rey, F. A. (2016). Structural basis of potent Zika-dengue virus antibody cross-
748 neutralization. *Nature, 536*(7614), 48-53. doi:10.1038/nature18938

749 46. Wang, Q., Yang, H., Liu, X., Dai, L., Ma, T., Qi, J., Wong, G., Peng, R., Liu, S.,
750 Li, J., Li, S., Song, J., Liu, J., He, J., Yuan, H., Xiong, Y., Liao, Y., Li, J., Yang, J.,
751 Tong, Z., Griffin, B. D., Bi, Y., Liang, M., Xu, X., Qin, C., Cheng, G., Zhang, X.,
752 Wang, P., Qiu, X., Kobinger, G., Shi, Y., Yan, J., & Gao, G. F. (2016). Molecular
753 determinants of human neutralizing antibodies isolated from a patient infected
754 with Zika virus. *Sci Transl Med, 8*(369), 369ra179.
755 doi:10.1126/scitranslmed.aai8336
756 47. Zhang, S., Kostyuchenko, V. A., Ng, T. S., Lim, X. N., Ooi, J. S., Lambert, S.,
757 Tan, T. Y., Widman, D. G., Shi, J., Baric, R. S., & Lok, S. M. (2016).
758 Neutralization mechanism of a highly potent antibody against Zika virus. *Nat*
759 *Commun, 7*, 13679. doi:10.1038/ncomms13679
760 48. Hasan, S. S., Miller, A., Sapparapu, G., Fernandez, E., Klose, T., Long, F.,
761 Fokine, A., Porta, J. C., Jiang, W., Diamond, M. S., Crowe, J. E., Jr., Kuhn, R. J.,
762 & Rossmann, M. G. (2017). A human antibody against Zika virus crosslinks the E
763 protein to prevent infection. *Nat Commun, 8*, 14722. doi:10.1038/ncomms14722
764 49. Robbiani, D. F., Bozzacco, L., Keeffe, J. R., Khouri, R., Olsen, P. C., Gazumyan,
765 A., Schaefer-Babajew, D., Avila-Rios, S., Nogueira, L., Patel, R., Azzopardi, S.
766 A., Uhl, L. F. K., Saeed, M., Sevilla-Reyes, E. E., Agudelo, M., Yao, K. H.,
767 Golijanin, J., Gristick, H. B., Lee, Y. E., Hurley, A., Caskey, M., Pai, J., Oliveira,
768 T., Wunder, E. A., Jr., Sacramento, G., Nery, N., Jr., Orge, C., Costa, F., Reis, M.
769 G., Thomas, N. M., Eisenreich, T., Weinberger, D. M., de Almeida, A. R. P.,
770 West, A. P., Jr., Rice, C. M., Bjorkman, P. J., Reyes-Teran, G., Ko, A. I.,
771 MacDonald, M. R., & Nussenzweig, M. C. (2017). Recurrent Potent Human

772 Neutralizing Antibodies to Zika Virus in Brazil and Mexico. *Cell, 169*(4), 597-609
773 e511. doi:10.1016/j.cell.2017.04.024
774

775 **Figures and Tables**

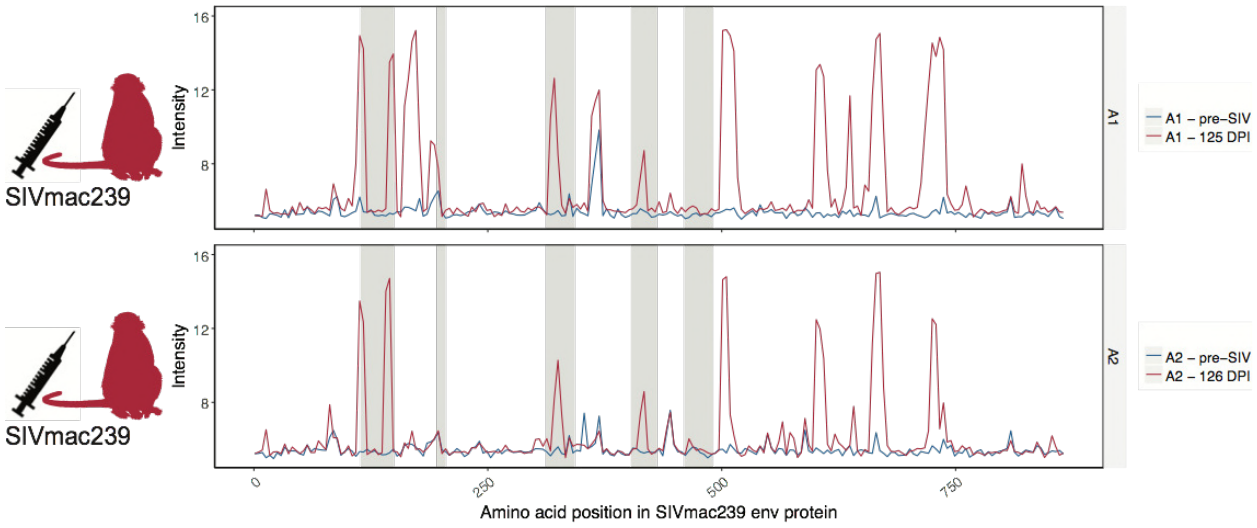

776

777 **Figure 1**: SIV env epitopes identified by a high-density peptide microarray overlap

778 known epitopes in variable loop regions. Serum from two cynomolgus macaques

779 (animals A1 and A2) before and after infection with SIVmac239 was evaluated for

780 reactivity to overlapping peptides representing the SIVmac239 env protein sequence on

781 a linear peptide microarray. SIV env variable loop regions (36) are highlighted in grey.

782

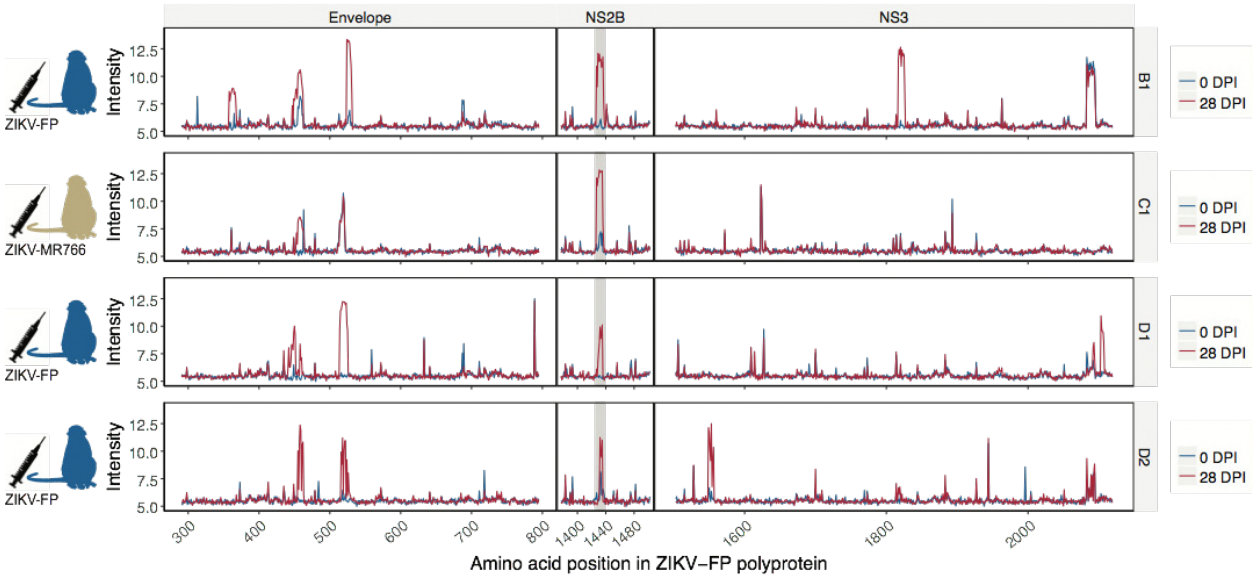

783

784 **Figure 2**: Reactivity of ZIKV-convalescent animals against the ZIKV-FP polyprotein.
785 Serum from rhesus macaques infected with ZIKV-FP (animals B1, D1, and D2) and
786 ZIKV-MR766 (animal C1) was assayed for IgG recognition of the ZIKV-FP polyprotein.
787 Reactivity at pre-infection and 28 dpi is shown. The $NS2B_{1427\text{-}1451}$RD25 epitope is
788 highlighted in grey. Using the mean signal intensity across this highlighted region, the
789 change of signal intensity from 0 dpi to 28 dpi was statistically significant versus no
790 change, by a two-tailed log-ratio t-test (p-value = 0.038 < 0.05, df = 3).
791

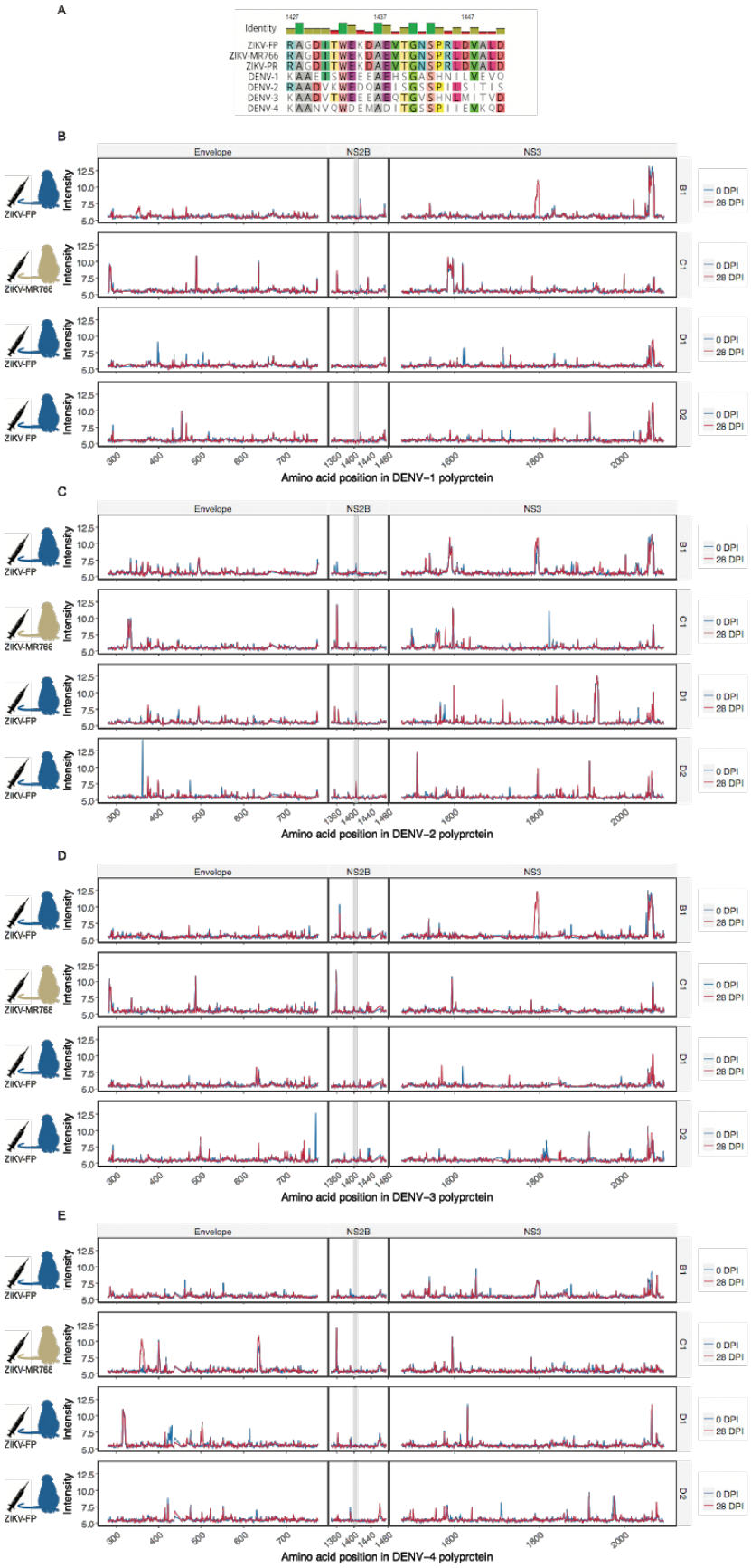
A
Identity
ZIKV-FP
ZIKV-MR766
ZIKV-PR
DENV-1
DENV-2
DENV-3
DENV-4
B
C
D
E
Envelope
NS2B
NS3
Intensity
B1
C1
D1
D2
0 DPI
28 DPI
Amino acid position in DENV-1 polyprotein
Amino acid position in DENV-2 polyprotein
Amino acid position in DENV-3 polyprotein
Amino acid position in DENV-4 polyprotein

792

793 **Figure 3**: Reactivity of ZIKV-convalescent animals against polyproteins of the four
794 DENV serotypes. DENV serotypes share an average of 41% sequence similarity with
795 the aligned ZIKV NS2B epitope (A). Serum from rhesus macaques infected with ZIKV-
796 FP (animals B1, D1, and D2) and ZIKV-MR766 (C1) was assayed for reactivity against
797 polyproteins of DENV serotypes 1-4 (B-E, respectively). The segment of DENV NS2B
798 which aligns with the ZIKV NS2B$_{1427\text{-}1451}$RD25 epitope is highlighted in grey.
799

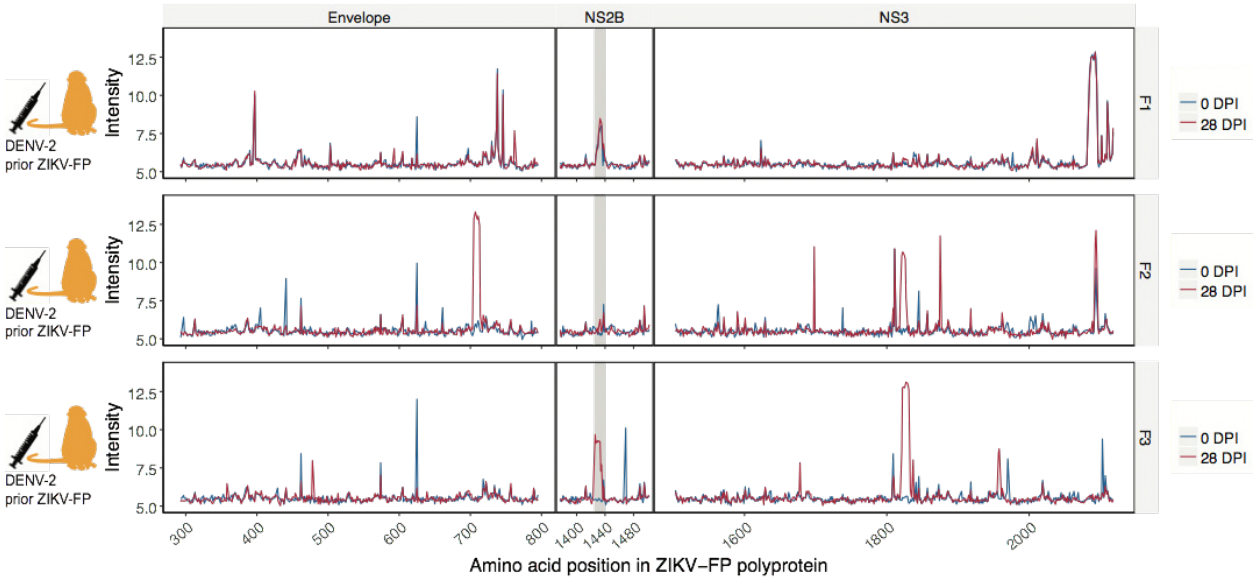

800

801 **Figure 4**: Antibody reactivity to the ZIKV NS2B epitope of animals with recent infection
802 with DENV. Three macaques (F1, F2, and F3) with history of challenge and re-
803 challenge with ZIKV-FP 12 and 9.5 months prior were infected with DENV-2 and their
804 serum was assessed before infection and at 28 dpi. The NS2B$_{1427\text{-}1451}$RD25 epitope is
805 highlighted in grey.
806

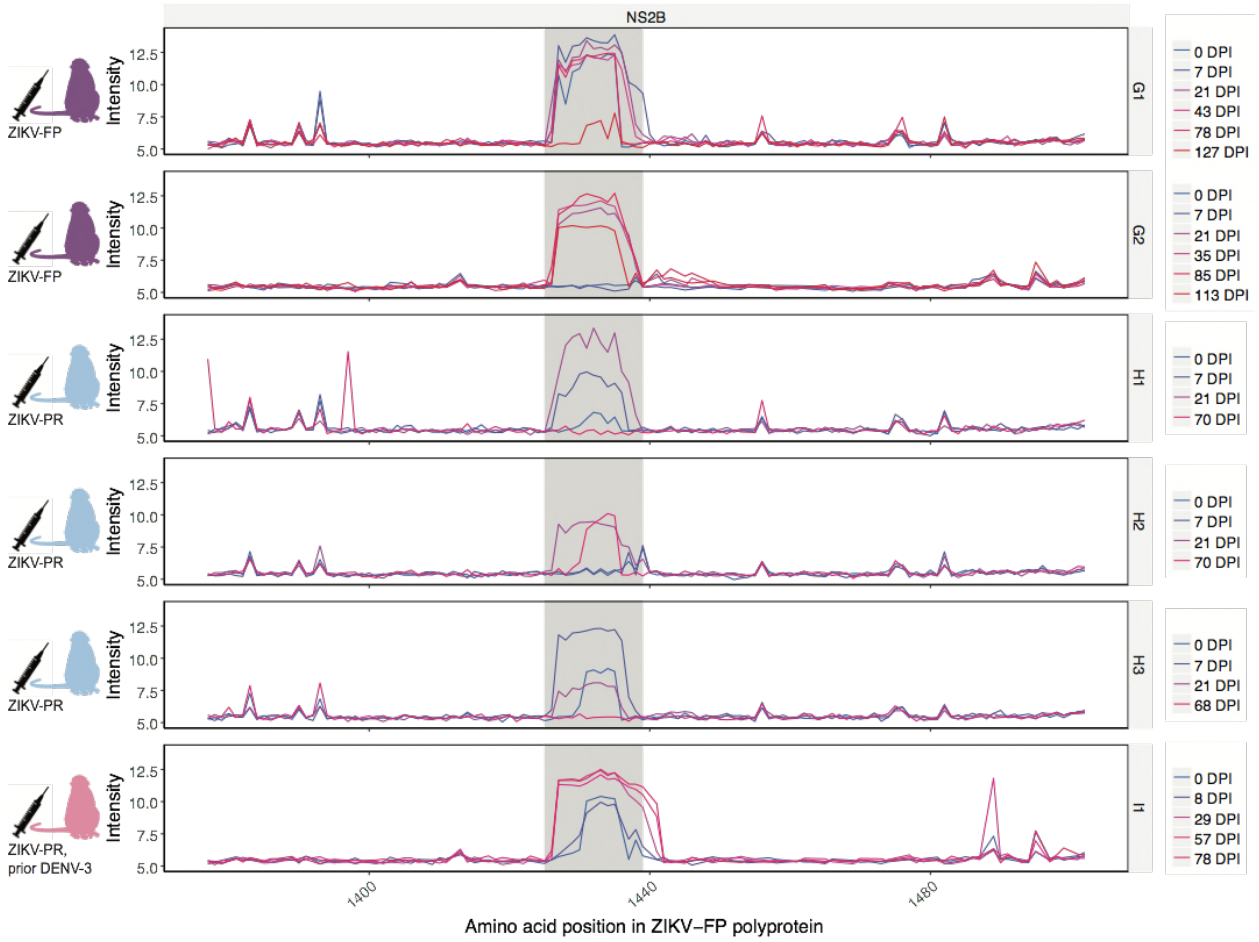

Figure 5: IgG reactivity against the ZIKV NS2B epitope during pregnancy. Serum samples taken throughout the course of six animals' pregnancies were evaluated against the ZIKV-FP polyprotein represented on peptide microarrays. Two animals (G1 and G2) were infected with ZIKV-FP at 36-38 gd. Three animals (H1, H2, H3) were infected with ZIKV-PR at 45-47 gd. One animal (I1) had been infected with DENV-3 nine months prior and was infected with ZIKV-PR at 35 gd. The $NS2B_{1427\text{-}1451}$RD25 epitope is highlighted in grey. Using the mean across this highlighted region, the change of signal intensity from 0 dpi to 21 or 29 dpi was statistically significant versus no change, by a two-tailed log-ratio t-test (p-value = 0.017 < 0.05, df = 5).

Table 1

Cohort	Animal	Public animal identifier*	Species	Sex	Flavivirus infection history	Inoculation strain	Inoculation dose and route	Time points of sample collection (days post infection, dpi)	Peptide array design
A	A1	cy0879	*Macaca fascicularis*	female	none	SIVmac239	7,000 TCID50, intrarectal	pre-infection, 125 dpi	Offset by 4, overlap of 12
	A2	cy0886	*Macaca fascicularis*	female	none	SIVmac239	7,000 TCID50, intrarectal	pre-infection, 126 dpi	Offset by 4, overlap of 12
B	B1	411359	*Macaca mulatta*	female	none	Zika virus/H.sapiens-tc/FRA/2013/FrenchPolynesia-01_v1c1	10E4 PFU, subcutaneous	pre-infection, 28, 67 and 99 dpi	Offset by 1, overlap of 15
C	C1	295022	*Macaca mulatta*	female	none	Zika virus/R.macaque-tc/UGA/1947/MR766-3329	10E4 PFU, subcutaneous	pre-infection, 28, 67 and 98 dpi	Offset by 1, overlap of 15
D	D1	448436	*Macaca mulatta*	male	none	Zika virus/H.sapiens-tc/FRA/2013/FrenchPolynesia-01_v1c1	10E4 PFU, subcutaneous	pre-infection, 28 and 621 dpi	Offset by 1, overlap of 15
	D2	861138	*Macaca mulatta*	female	none	Zika virus/H.sapiens-tc/FRA/2013/FrenchPolynesia-01_v1c1	10E4 PFU, subcutaneous	pre-infection, 28 and 582 dpi	Offset by 1, overlap of 15
F	F1	393422	*Macaca mulatta*	male	Zika virus/H.sapiens-tc/FRA/2013/FrenchPolynesia-01_v1c1, 12 and 9.5 months prior	Dengue 2 New Guinea C	10E5 PFU, subcutaneous	pre-infection, 28 dpi	Offset by 4, overlap of 12
	F2	826226	*Macaca mulatta*	male	Zika virus/H.sapiens-tc/FRA/2013/FrenchPolynesia-01_v1c1, 12 and 9.5 months prior	Dengue 2 New Guinea C	10E5 PFU, subcutaneous	pre-infection, 28 dpi	Offset by 4, overlap of 12
	F3	912116	*Macaca mulatta*	male	Zika virus/H.sapiens-tc/FRA/2013/FrenchPolynesia-01_v1c1, 12 and 9.5 months prior	Dengue 2 New Guinea C	10E5 PFU, subcutaneous	pre-infection, 28 dpi	Offset by 4, overlap of 12
G	G1	660875	*Macaca mulatta*	female	none	Zika virus/H.sapiens-tc/FRA/2013/FrenchPolynesia-01_v1c1	10E4 PFU, subcutaneous	pre-infection, 7, 21, 43, 78, 127 dpi	Offset by 1, overlap of 15
	G2	827577	*Macaca mulatta*	female	none	Zika virus/H.sapiens-tc/FRA/2013/FrenchPolynesia-01_v1c1	10E4 PFU, subcutaneous	0, 7, 21, 35, 71, 113 days after primary infection	Offset by 4, overlap of 12
H	H1	146523	*Macaca mulatta*	female	none	Zika virus/H.sapiens-tc/PUR/2015/PRVABC59	10E4 PFU, subcutaneous	pre-infection, 7, 21, 70 dpi	Offset by 1, overlap of 15
	H2	858972	*Macaca mulatta*	female	none	Zika virus/H.sapiens-tc/PUR/2015/PRVABC59	10E4 PFU, subcutaneous	pre-infection, 7, 21, 70 dpi	Offset by 1, overlap of 15
	H3	419969	*Macaca mulatta*	female	none	Zika virus/H.sapiens-tc/PUR/2015/PRVABC59	10E4 PFU, subcutaneous	pre-infection, 7, 21, 70 dpi	Offset by 1, overlap of 15
I	I1	776301	*Macaca mulatta*	female	Dengue 3 Slenman/78, 9 months prior	Zika virus/H.sapiens-tc/PUR/2015/PRVABC59 bar code virus	10E4 PFU, subcutaneous	pre-infection, 8, 29, 57, 78 dpi	Offset by 4, overlap of 12

*Public animal identifiers are used in studies on the Zika Open Research Portal (https://zika.labkey.com/project/home/begin.view?).

Table 2

Animal	Gestational days (gd) at inoculation	Pregnancy outcome
G1	36	delivery at 158 gd (122 dpi)
G2	38	delivery at 158 gd (120 dpi)
H1	46	fetectomy at 116 gd (70 dpi)
H2	47	fetectomy at 117 gd (70 dpi)
H3	43	fetectomy at 111 gd (68 dpi)
I1	35	delivery at 155 gd (120 dpi)